Periodic Orbits, Bifurcation Diagrams and the Spectroscopy of C_2H_2 System

R. Prosmiti and S. C. Farantos

Institute of Electronic Structure and Laser,

Foundation for Research and Technology Hellas, and

Department of Chemistry,

University of Crete,

Iraklion, Crete 711 10, Greece

Abstract

The principal families of periodic orbits that emerge from the stationary points of the six dimensional potential energy surface of C_2H_2 molecular system, as well as periodic orbits from saddle-node bifurcations have been located and propagated for an energy range up to 36500 cm^{-1} above the absolute minimum of the potential. The bifurcation diagrams of these periodic orbits reveal the regions of phase space where the dynamics are regular or chaotic (with soft or hard chaos) for acetylene, vinylidene, and the region over these two isomers. An association of the structure of phase space with spectroscopic findings is made by calculating Gutzwiller's semiclassical trace formula and classical survival probability functions.

1 Introduction

The study of vibrationally highly excited polyatomic molecules is a field of intensive research for the experimental and theoretical spectroscopy,[1–3] and acetylene is one of a few molecules for which detailed spectroscopic results exist.

The vibrational spectroscopy of acetylene in the electronic ground state ($X^1\Sigma_g^+$) has extensively been studied by Field and collaborators.[4,5] One of the reasons for that is the association of this molecule with the studies of vibrational chaos.[6] Using dispersed fluorescence (DF) and stimulated emission pumping (SEP) spectroscopy, vibrational spectra have been recorded with low and high resolution covering an energy range up to about 28000 cm^{-1}. The spectroscopic transitions involved single rovibrational levels of the A^1A_u electronic state. The high resolution SEP spectra near 27900 cm^{-1} revealed levels which satisfy some of the criteria of quantum chaos, such as the Wigner distribution of the energy differences between adjacent energy levels,[6–8] and the statistical Fourier transform analysis.[9,10]

Contrary to that, low resolution spectra show peaks which can be assigned with approximate quantum numbers related to the vibrational normal modes of the molecule. By increasing the resolution each peak is resolved to more peaks which may also be labeled by approximate quantum numbers. The clumps observed in the low resolution DF spectra have been named by Yamanouchi et al.[4] **feature states**.

Feature states are not single eigenstates of the molecule but a collection of them. Yamanouchi et al.[4] assigned most of the feature states in their spectra as progressions of the CC stretch and *trans* bend normal modes. To understand these regularities in low resolution spectra it is better to adopt a time domain formalism for vibrational spectroscopy.[11] Then, low resolution means that the wave packet which describes the initial excitation evolves for short time, whereas high resolution implies long time dynamics for the molecule. The clump structures observed in the DF spectra is the result of recurrencies of the wave packet at the region in the coordinate space where it started. The fact that the clumps are labeled with normal mode quantum numbers means, that the eigenstates in which the wave packet is analyzed overlap with the same region, and their superposition gives regular structures.

Direct absorption spectra of acetylene on the ground electronic state have also been recorded with the optoacoustic laser intracavity method[12] up to 23000 cm^{-1}, as well as with Fourier transform spectrometers.[13,14] These spectra have been assigned with mainly CH stretch vibrational modes quantum numbers (normal or local). Again, the assignment of the spectral lines imply regular and localized eigenfunctions at energies where SEP spectroscopy predicts chaotic behavior. With this observation Smith and Winn[14] concluded that acetylene has a phase space which accommodates regular and chaotic regions for the same energy interval.

It is really impressive to see that even at such high excitations, where the non linearity of the potential significantly increases, traditional approaches, such as normal mode zero order hamiltonians plus perturbation methods, are successful. This poses the problem of understanding better the dynamics of acetylene.

A number of quantum mechanical calculations that involve a three dimensional (3D) stretch mode hamiltonian,[15] a coplanar 5D hamiltonian,[16,17] and a full 9D vibrational rotational hamiltonian[18] have been reported. All these calculations gave vibrational levels lower than 10000 cm^{-1} with the exception of the 3D calculations which go up to 20000 cm^{-1}. The experimental spectra of the highly excited molecule still lack a theoretical explanation.

Unequivocally, there is a substantial progress in the quantum mechanical calculations as the above results demonstrate, and that is due to the development of the grid methods,[19] and of course to the new technology fast computers. Nevertheless, dealing with highly energized polyatomic molecules quantum mechanical calculations are still difficult to perform even for triatomic molecules.

Classical mechanics in the regime of validity of the semiclassical approximation circumvent the problems of dimensionality and the range of excitation in the molecules. On the other hand, highly energized molecules bring new problems because of the non linear effects encountered at high energies. Thus, concepts and methods of non linear classical mechanics must be employed to extract the dynamics from experimentally observed quantities.[1,3]

The good agreement between classical and quantum dynamics on model and realistic systems[20] found up to now motivates one to use classical non linear mechanics to explore the dynamics of a molecule, and to associate them with spectroscopic results. For example, in the frame of non linear mechanics localization of the wave functions and regularities in the spectra may be related with regions in phase space where the motion is regular or governed by unstable periodic orbits.[21,22]

Holme and Levine[23,24] carried out classical trajectory calculations on a model potential function trying to simulate the SEP spectroscopy of acetylene. They proposed that the two time scales found in the statistical Fourier transform analysis correspond to the stepwise energy flow from CH stretches to the CC stretch and then to *trans* bend. Jonas et al.[5] have argued that the energy flow is through resonances of *cis/trans* bend and CC stretch vibrational modes.

Early work by one of us[25] showed that the phase space of C_2H_2 at about 28000 cm^{-1} is mainly chaotic, but some regions with small positive Lyapunov characteristic exponents exist and can trap the trajectories. In the following years we found, that a systematic way to reveal the structure of phase space, and thus the related dynamical behavior of the molecule, is achieved by constructing continuation/bifurcation diagrams of periodic orbits[26] that originate from the stationary points of the molecular potential energy surface.[27] Most of this work has been done for two and three degrees of freedom model molecular potentials.[20,28–32]

We think that up to now there is no systematic analysis of the classical mechanical behavior of acetylene in the range of energies now accessible to spectroscopists. Hence, the purpose of the present article is twofold. First, we like to extend our techniques and algorithms of periodic orbit analysis to polyatomic molecules. Acetylene is a proper choice for applying these techniques, since analytical potential functions, experimental results, and quantum mechanical calculations are available. Therefore, the second goal of this work is to interpret in a qualitative way some of the spectroscopic results in terms of the periodic orbits of the system. The connection of particular phase space structures with spectroscopy is done by computing Gutzwiller's trace formula,[6] and by evaluating the classical survival probability function.[1]

2 Methods for Locating Periodic Orbits

The molecular potential energy surfaces are not only multidimensional but also complicated analytical functions. Thus, numerical techniques must be employed in order to find the periodic solutions of Hamilton's equations of motion.

If $\vec{x}$ denotes the vector of all coordinates, $q_1, q_2, ..., q_N$, and their conjugate momenta, $p_1, p_2, ..., p_N$, of a molecule of N degrees of freedom, then to find the initial conditions of a periodic orbit it is necessary to search for the roots of the non linear system,

$$\vec{x}(T) - \vec{x}(0) = 0. \tag{1}$$

$\vec{x}(0)$ is the initial point in phase space and $\vec{x}(T)$ the point after integrating Hamilton's equations of motion for one period of time, T.

This is a *2-point boundary value problem* and it is converted to an *initial value problem* by considering the initial conditions of the coordinates and momenta $\vec{s}$

$$\vec{x}(0) = \vec{s}, \tag{2}$$

as independent variables of the non linear functions

$$\vec{B}(\vec{s}) = \vec{x}(T; \vec{s}) - \vec{s}. \tag{3}$$

We denote the roots of Eq. (3) as $\vec{s}_*$, i.e.,

$$\vec{B}(\vec{s}_*) = 0. \tag{4}$$

Hence, if $\vec{s}$ is a nearby value to the solution $\vec{s}_*$ we can compute the functions $\vec{B}(\vec{s})$ by integrating Hamilton's equations for the period T (the shooting technique). By appropriately modifying the initial values $\vec{s}$ we hope to converge to the solution, that is, $\vec{s} \to \vec{s}_*$ and $B \to 0$. The common method to find the roots of equation (4) is the Newton-Raphson.[33]

The Newton-Raphson method is an iterative scheme and at each iteration, k, we update the initial conditions of the orbit

$$\vec{s}_{k+1} = \vec{s}_k + \Delta\vec{s}_k. \tag{5}$$

The corrections $\Delta\vec{s}_k$ are obtained by expanding $\vec{B}(\vec{s})$ in a Taylor series up to the first order, and then, we solve the linear algebraic equations

$$[Z_k(T) - I_{2N}]\Delta\vec{s}_k = -\vec{B}(\vec{s}_k). \tag{6}$$

$Z_k(T)$ is the fundamental matrix and is evaluated by integrating the variational equations

$$\dot{\vec{z}}(t) = J\partial^2 H[\vec{x}(t)]\vec{z}(t). \tag{7}$$

$\partial^2 H[\vec{x}(t)]$ denotes the matrix of the second derivatives of the hamiltonian computed at $\vec{x}(t)$. The initial values of $\vec{z}(0)$ are the vectors (1,0,...,0), (0,1,0,...,0),..., (0,0,...,1), and the result of the integration gives the matrix $Z(T)$ whose columns are the vectors $z(\vec{T})$.[26,34] J is the symplectic matrix

$$J = \begin{pmatrix} 0_N & I_N \\ -I_N & 0_N \end{pmatrix}. \tag{8}$$

0_N and I_N are the zero and unit $N \times N$ matrices respectively.

The system of linear algebraic equations (Eq. 6) is solved using LU decomposition algorithms. In cases where the matrix of coefficients is ill-conditioned we use Singular Value Decomposition (SVD) methods.[33] The fundamental matrix is computed either by integrating simultaneously Hamilton's and variational equations, when the analytical second derivatives of the hamiltonian are available, or by finite differences from two neighboring trajectories which are integrated for time T.

The above method is frequently called simple shooting method. As we have recently demonstrated[35] the multiple shooting method is a much more powerful technique, especially for highly unstable systems, and it is applied in the cases where simple shooting fails.

The Hamilton's equations of motion for acetylene and in general for tetratomic molecules have been expressed in several coordinate systems. First, we use the hamiltonian proposed by Bentley et al.[16] in their quantum mechanical calculations. In this article the authors ignore the out of plane coordinate and a term in the hamiltonian which makes a small contribution to the eigenenergies. To include the out of plane motion we use a 6D hamiltonian in Jacobi coordinates or a diatom-diatom hamiltonian.[36] Finally, a 9D hamiltonian that may describe rotations as well, has been constructed by using Jacobi coordinates in a cartesian space and subtracting the coordinates of the center of mass. In the Appendix we have tabulated the hamiltonians that are commonly used to study tetratomic molecules. The different coordinate systems and the associated zero order Hamiltonians facilitate our task to find good starting points in the Newton-Raphson process.

The potential energy surface for the electronic ground state of C_2H_2 which we employ,[37] is the same with that which we used in our previous work.[25] The same potential function was also used by Bentley et al.[16] and other investigators. The minimum of acetylene is of linear geometry and of energy -17.552 eV, with the zero of energy defined for the four atoms separated and in their gound electronic state. Vinylidene is at -15.838 eV and with a C_{2v} geometry. The transition state is at -15.469 eV and with an asymmetric configuration.

In the periodic orbits search we first locate the principal families, those which originate from the stationary points of the potential. It is quite easy to locate them since they are associated with the normal modes of the molecule.[38,39] Then, we follow the evolution of these periodic orbits by slowly increasing the total energy or equivalently, by varying the period of the periodic orbits. During this process bifurcating families of periodic orbits are obtained and the stability properties of the family are examined. These results are then used to construct continuation/bifurcation diagrams, i.e., plots of the initial conditions of the periodic orbits with the varying parameter. Such diagrams portrait basic features of the structure of phase space. Details about the methods that we use are reviewed in previous publications.[3,27]

The stability properties of a periodic orbit are determined by examining the eigenvalues of the monodromy matrix, i.e., the fundamental matrix computed for the periodic orbit and integrating the equations of motion for one period T. Since, we are dealing with a conservative hamiltonian system the eigenvalues are always pairs of complex conjugate numbers or pairs of real inverse numbers. Furthermore, one pair is always equal to one.

A periodic orbit is stable when all the eigenvalues of monodromy matrix lie on the unit complex circle. Instability appears when one or more pairs of the eigenvalues come out of the unit circle. In the case of complex instability the symplectic properties of the hamiltonian systems imply that two pairs of eigenvalues are related as $(\lambda, 1/\lambda, \lambda^*, 1/\lambda^*)$, where λ and λ^* are complex conjugate. Complex instability occurs in systems with more than two degrees of freedom, and its correspondence to quantum mechanics constituted the subject of a recent investigation.[40]

Thus, for a multidimensional system there are several types of instability. To describe them we shall denote with S those pairs of eigenvalues that are unit complex, with U pairs of inverse real numbers, and Δ quadruplets of complex eigenvalues out of the unit circle. For a 5D system we have 5 pairs of eigenvalues computed by diagonalizing the monodromy matrix. Excluding the pair which is always equal to one, we may have the following types of instabilities: single, double, triple, quadruple, complex, and combinations of complex with single and double instability. Double complex instability is also possible, and we give an example later on. Symbolically, the above cases are described as

SSSS, USSS, UUSS, UUUS, UUUU, ΔSS, ΔUS, ΔUU, ΔΔ.

3 Bifurcation Diagrams

Most of the periodic orbits lie in reduced dimension spaces, therefore we have used extensively in the periodic orbit search the 5D hamiltonian for the in plane motions given in the Appendix (Eq. A1). The coordinate system and their symbols are described in Fig. A1 of the Appendix. For the out of plane periodic orbits the Jacobi coordinate system and the hamiltonians Eqs A2 and A3 are employed. For energy units we use both wavenumbers and electronvolts (1 eV = 8065.541 cm^{-1}).

3.1 Bifurcation diagram of acetylene

Figure 1 shows a projection of the bifurcation diagram of C_2H_2 in the (E, p_{r_1}) plane. p_{r_1} is the momentum conjugate to the distance of hydrogen atom 1 from the center of mass of CC diatom. We chose this projection since it presents better the continuation of the families of periodic orbits avoiding intersections during their projections. Each curve corresponds to a family of periodic orbits, and is related with one of the normal modes of the molecule. This is deduced from Weinstein's theorem,[38] which states that from the minimum of the potential function emanate at least as many periodic orbits as the number of normal modes. Thus, we label the principal families of periodic orbits as symmetric stretch (SS), antisymmetric stretch (AS), carbon carbon stretch (CC), *trans* bend (TR) and *cis* bend (CIS). The degenerate bend modes correspond to two equivalent principal families of periodic orbits which lie on the (x, z) and (y, z) planes respectively. This has been confirmed by locating these periodic orbits in the cartesian coordinate system and using the 9D hamiltonian (Eq. A2). We must point out that the conjunction of principal families with normal modes does not imply that normal mode description of the motions is valid at high energies. On the contrary, the morphologies of periodic orbits may vary significantly with the energy.

Each point on a curve in the bifurcation diagram denotes the initial conditions of the periodic orbit at energy E. Continuous lines mean that the periodic orbits are stable. Dotted lines signal that the stability of periodic orbits has changed to single unstable, that is, the motion in one degree of freedom has become unstable. The open circles mark double unstable periodic orbits and the crosses complex instability. The triple instability will be represented with diamonds. We have not found quadruple instability: four pairs of real eigenvalues.

Table I gives initial conditions for representative periodic orbits of acetylene found in this work. The final column shows the stability properties of the periodic orbit at that particular energy. In Fig. 2 we plot a few periodic orbits of acetylene projected in the (r_1, θ_1) plane.

Daughter families which bifurcate from the principal or previous bifurcations are also shown in Fig. 1 and are coded in such a way that we can trace their generation. For example, the code TR1A1A describes the family that bifurcates from the first bifurcation of the TR principal family and from the branch A. Bifurcating periodic orbits may have the same period with the parent one or double and even multiple periods. Once we found one periodic orbit of each family, starting from the minimum of the potential, the construction of the bifurcation diagram presented no difficulties.

A striking outcome emerges from Fig. 1. The shown bifurcation diagram covers an energy range of 36500 cm^{-1} and with the exception of the AS family all other principal families of periodic orbits are stable for a substantial range of energies. The symmetric stretch (SS) is stable for the whole energy range. The *trans* bend family, (TR), turns to single unstable at 23200 cm^{-1} above the minimum, then becomes stable again, and eventually turns to double unstable. We can see early bifurcations of TR (TR1A, TR2A). We have found that one pair of eigenvalues of the *trans* family approaches unity for several times and without changing its stability. This means that new families appear from the TR with the same period. The CIS family remains stable for most of the studied energy interval, and the CC family changes stability at 29185 cm^{-1}. The bifurcating families, AS1A and AS1B, from the AS are generated stable and with the same period, but become complex unstable (ΔSS) at the energy

18850 cm^{-1} above the absolute minimum.

We may conclude that the periodic orbit analysis reveals stable regions in the phase space of acetylene 36500 cm^{-1} above the minimum. We emphasize that single instability means instability only in one degree of freedom and stability in all others. Thus, it is not introduced strong chaos by turning the periodic orbits to single unstable. The largest real eigenvalue of the monodromy matrix did not exceed the value of 77 in the studied range of energies.

3.2 Bifurcation diagram of vinylidene

In Fig. 3 the bifurcation diagram of vinylidene is shown. Table IIa tabulates the initial conditions of representative periodic orbits of each family, and Table IIb gives the initial conditions for the out of plane periodic orbit in the Jacobi 6D coordinate system. Figure 4 presents the morphologies of some periodic orbits projected in the (r_1, θ_1) plane.

The correspondence of the principal families to normal vibrational modes is: VSS for the symmetric stretch, VAS for the antisymmetric stretch, VCC for the carbon carbon stretch, and the ROCK, SCIS and OUT for the rock, scissor, and out of plane bend motions respectively.

Looking at the stability of the principal families we immediately notice the frequency of appearance of complex instability. The family which corresponds to the rock normal type of motion becomes complex unstable at about 16905 cm^{-1} above the absolute minimum, and although it turns to stable, double and triple unstable for short energy intervals, it remains complex unstable for most of the energies. The VSS family also turns from stable to complex unstable at about 19478 cm^{-1}. However, the antisymmetric stretch, VAS, and the scissor, SCIS, families are stable for a substantial range of energies. The VAS becomes single unstable and returns to stable again at 31283 cm^{-1} above the absolute minimum. The VCC family also shows extended regions of stability. Finally, the out of plane principal family of vinylidene remains stable up to 28691 cm^{-1}, and turns to single unstable for an energy range of 2702 cm^{-1}, and then becomes stable again.

We may conclude from the stability analysis of the principal families of vinylidene that its phase space is less stable than that of acetylene, but still, regular motions are expected around the stable periodic orbits in spite of the high energy regions that we examine.

3.3 Periodic orbits of the transition state and saddle-node bifurcations

Figure 5 shows the continuation diagram in the (E, r_1) plane for the principal families that emerge from the saddle point of the potential function. We know from Moser's theorem[39] that for a 6D system five principal families originate from a saddle point, while the 6th degree of freedom corresponds to the unstable direction. Since the configuration of the transition state is asymmetric we label the principal families as TSA, TSB, TSC, TSD, and the out of plane as TSOUT. Initial conditions for representative periodic orbits are given in Table III, and plots of trajectories in Fig. 6.

As is expected the instability of the region is reflected in the stability properties of the periodic orbits. All families start as single unstable and later become complex, double, and even triple unstable. The out of plane periodic orbit of the transition state remains single unstable up to 18513 cm^{-1}, and after that it becomes complex unstable (ΔSS). The TSD family presented difficulties in the continuation step.

Periodic orbits which may connect the regions of two different minima of the potential energy surface originate from saddle-node bifurcations. We have searched for this type of periodic orbits using the 5D hamiltonian. To avoid confusion we state that saddle-node bifurcating periodic orbits are different from those that emerge from the saddle point of the potential function. Figure 7 portraits the continuation/bifurcation diagram of the saddle-node periodic orbits. These periodic orbits describe full rotations of hydrogen atoms around the CC diatomic molecule, and thus, we label them with R from the rotating. At the saddle-node bifurcation point two families emerge simultaneously and are denoted as A and B. Bifurcating families of first and second generation are also shown.

It is difficult to symbolize the stability of these periodic orbits on one diagram, because of their frequent alterations as energy increases. Thus, to distinguish the two branches we use continuous and dash lines without referring to their stability. In Table IV we give initial conditions of some periodic orbits, their energies, periods, and the stabilities at that particular energy. In Fig. 8 we plot representative periodic orbits.

In 2D systems saddle-node bifurcations emerge always in two branches; one with stable periodic orbits and one with unstable. It is interesting to note that in multidimensional systems there may be different combinations. In table V we tabulate the energy of appearance, the period, and the stability of the emerging periodic orbits. Only the R2 families start as stable and single unstable, whereas the combinations for the others vary. The characteristics of the saddle-node bifurcations found in two degrees of freedom systems remain the same for the multidimensional case. That is, bifurcation occurs when one pair of eigenvalues becomes equal to one with degenerate eigenvectors, and the period in one branch increases and in the other decreases.

We could imagine more than one pairs of unit eigenvalues, and thus, more than one pairs of bifurcating saddle-node periodic orbits from a single point in phase space. However, we have not located such a case in this work.

The stability analysis of the saddle-node periodic orbits reveals a generally unstable region in phase space. From the lower energy saddle-node bifurcations, R1 and R2, periodic orbits emerge with periods about 12 t.u. (1 t.u. = 1.018×10^{-14} sec), and with a rather complex morphology, because of the oscillations in the acetylene minimum (Fig. 8). The higher energy saddle-node bifurcations are of simpler form and of smaller periods.

The R3B2A family shows double complex instability for the energies 31012 - 33288 cm^{-1}. That means that there are two sets of quadruplet eigenvalues out of the unit complex circle. In Fig. 9 we plot the eight eigenvalues for the energy range (28555-33288) cm^{-1}. One set takes large values (and their inverse eigenvalues small) and we can see their collision on the real axis (indicated in Fig. 9a with an arrow) as the family turns from double unstable to complex unstable. Figure 9b magnifies the region in the center and we can see the collisions of the other quadruplet of eigenvalues as they move on the unit complex circle with the energy, and how they come out of this circle (indicated in Fig. 9b with the arrows).

In previous work[41] we have emphasized that saddle-node bifurcations connect different minima on the potential energy surface, and bring stability in the phase space of the molecule at high energies through the stable branch. Although the rotational periodic orbits of C_2H_2 system have frequent changes in their stability, we have found that some of them remain stable or single unstable for appreciable energy intervals.

4 Classical Survival Probability Functions

It is not unjustifiable to claim that a periodic orbit tree is the skeleton of phase space. However, linear stability analysis can not tell us the size of the region that is influenced by a periodic orbit. A way to have an estimate of the neighborhood that is influenced by a periodic orbit in multidimensional systems is to run batches of trajectories selected around the periodic orbit at a particular energy and according to some distribution function.

We have found that the classical analogue of the quantum mechanical survival probability function serves this purpose. The classical time autocorrelation function, $C(t)$, has successfully been used to simulate experimental spectra.[20,42–44] Here, we compute this function considering these calculations as computer experiments with a Gaussian initial distribution launched on a periodic orbit at a particular energy.

The results for acetylene are shown in Figs. 10 and 11 at two energies, 20543 cm^{-1} and 28689 cm^{-1} respectively, and using 2000 trajectories to obtain converged values of the autocorrelation function $C(t)$. The width of the initial Gaussian distribution is chosen such as most of the selected trajectories have energies ranging in an interval $\pm$ 4000 cm^{-1} around the peak energies given above. The labels in each frame in the figures is the label of the periodic orbit on which the initial distribution is centered.

With the exception of the correlation functions centered on the *trans* type periodic orbits the other show regularities for both energies studied. The time between two adjacent peaks corresponds to the period of the periodic orbit. Although the recurrencies of the *trans* autocorrelation functions agree with the periods of the *trans* periodic orbits the low intensities and the complexity of these peaks are in accordance with the continuation/bifurcation pattern of the family. As we stated it before the *trans* family has many bifurcating periodic orbits with similar periods, which obviously give the structure in the peaks of the autocorrelation functions.

The region of phase space around the TR1A2A1A family marks the position of an initial wave packet which is originated from the upper electronic state[45] that is used in the SEP experiments. *Trans* progressions are expected in the spectrum and this is what is revealed from the time autocorrelation function.

The results of the periodic orbit analysis and of the classical survival probability functions support the conclusion that *acetylene is more regular than we thought before.*

Regular survival probability functions are also computed for vinylidene at the energy of 20543 cm^{-1}, Fig. 12. The most complex pattern is that of the ROCK periodic orbit, a family which shows an early transition to complex instability (Fig. 3).

Fig. 13 presents the results of two Gaussians centered on the rotating type periodic orbits at energies 20543 cm^{-1} for the R1A periodic orbit and 28689 cm^{-1} for the R3A. In these figures we can trace recurrences at the periods of the rotating periodic orbit, but the rich structure demonstrates that the region of phase space is occupied by many periodic orbits. In the case of R3A we found that many sampled trajectories are influenced by bifurcating periodic orbits of the TR family.

5 Partial Summation of Gutzwiller's Trace Formula and Feature States

Gutzwiller[6] has produced a semiclassical formula to calculate the density of states of a dynamical system based on periodic orbits;

$$D(E) = D_{av}(E) + N(E), \tag{9}$$

$$N(E) = Re \sum_{po} \frac{T_{po}}{\pi\hbar} \sum_{j=1}^{\infty} \frac{\exp[ij(S_{po}/\hbar - \mu_{po}\pi/2)]}{[det(M_{po}^{j} - 1)]^{1/2}}. \tag{10}$$

$D(E)$ is the density of states at energy, E, and $D_{av}(E)$ is the average value of it. $N(E)$ describes the fluctuations of the density of states around D_{av}, and the calculation of $N(E)$ requires a summation over all periodic orbits with period T_{po}, action S_{po}, as well as a summation over an infite number of loops. μ_{po} is the Maslov index and M_{po}^{j} is the stability matrix which describes the results of the transverse displacements off the periodic orbit after j loops. It is computed directly from the eigenvalues of the monodromy matrix

$$det(M_{po}^{j}-1)=\prod_{i=1}^{2(N-1)}(\lambda_{po}^{j}(i)-1), \tag{11}$$

where $\lambda_{po}^{j}(i)$ is the jth power of the ith eigenvalue (a complex or real number) of the monodromy matrix which corresponds to a perpendicular direction of the periodic orbit. The use of the monodromy matrix in the trace formula implies that a linear approximation is introduced to describe the motions in the neighborhood of the periodic orbit.

The task of carrying out the two summations in Eq. (10) seems formidable for one to apply this equation, and even more, it has raised a lot of criticism[46–48] in the literature about its convergence. Nevertheless, applications of Gutzwiller's equation demonstrate that even using a limited number of periodic orbits, the isolation of a few quantum mechanical states is achieved.[49, 50]

To cope with the convergence of the trace formula with respect to j, Berry and Tabor[46] and others[6, 50] have suggested to multiply the terms in the sum with the smoothing function

$$f(E)=\exp\left[-\frac{\gamma j T_{po}(E)}{\hbar}\right], \tag{12}$$

where $\gamma>0$ is a decay parameter. This means that a finite resolution of the lines is introduced. Still, the problem of showing that the spectral lines do not vary by increasing the number of periodic orbits remains.

It is apparent that all the ingredients of the trace formula are computed for specific families during the construction of the continuation/bifurcation diagram. Therefore, we believe that it is interesting to calculate the trace formula and check its performance for a multidimensional system such as acetylene.

The success of this equation or various versions of it in including only a finite number of periodic orbits certainly relies on the assumption that the eigenfunctions are localized or overlap with these periodic orbits. Under this assumption we analyze the fluctuations of the density of states of acetylene in terms of specific periodic orbits. However, since it is difficult to extract individual eigenlevels at high energies, we assume that the fluctuations are broad features of the acetylene spectrum, and thus we compare them with the feature states of Yamanouchi et al.[4]

In Fig. 14 we show the quantity $N(E)$ for acetylene computed by using the five principal families of periodic orbits shown in Fig. 1. The vertical lines at the top of the figure mark the energy positions of the feature states fitted by Yamanouchi et al.[4] To avoid misunderstandings we repeat that the stick spectrum does not correspond to eigenlevels of acetylene, but they mark the position of broad peaks under which hundreds of lines may be hidden. The feature states have been assigned as progressions of the CC stretch quantum number $m, (m = 0-8)$, and the *trans* bend quantum number $n, (n = 0-18)$. We do not give the assigned numbers here, but it is clear that the semiclassical results do not give the proper resolution seen in the experimental spectrum.

Recalculating Eq. (10) using only the CC stretch and *trans* bend families of periodic orbits the spectrum shown in Figure 15 is produced. This graph may be compared with the part of Fig. 14 in the same energy interval, and we see no significant differences (the intensities are arbitrary). The stars in the figure denote the positions of the peaks which are obtained when we use only the CC family.

At the top of figure 15 the vertical lines mark the energy positions produced by Yamanouchi et al.[4] for the feature states. Their assignment is also given. From this stick spectrum a low resolution one is produced using Gaussian smoothing functions centered at the fitted energies.

We think that it is eligible to compare the two spectra since the semiclassical estimates are the results of periodic orbits which describe CC stretch and *trans* bend types of motion in the molecule. Although it is difficult to establish an exact correspondence of the assigned features with the fluctuations of the density of states, we can see that progressions in the *trans* bend mode are represented in the semiclassical results.

Comparing the computed semiclassical peaks using an analytical potential function with those of Yamanouchi et al., we should take in account that the energy gap between two consecutive peaks is about 700 cm^{-1} which is a little bit higher than the energy difference of two consecutive *trans* feature states (divided by 2). The same is true for the CC feature states; the energy gap is about 1870 cm^{-1}. Also, the semiclassical formula predicts both even and odd *trans* states.

The above analysis lead to the conclusion that the partial summation of Gutzwiller's formula applied with a few families of periodic orbits of well characterized molecular motions may reveal spectroscopic features seen under low resolution.

6 Conclusions

The appearance of regularities in low resolution spectra of polyatomic molecules seems to be the general trend. Traditional perturbative techniques with a zero order hamiltonian in normal or local coordinates, as well as new techniques such as the hierarchical method of Davis[51] are used to assign these spectra, and thus, to reveal the dynamics of the molecule. Periodic orbit analysis through continuation/bifurcation diagrams offers an alternative method.

Acetylene is the first molecule for which quantum chaos was detected. Even more, for this molecule experimental spectroscopy has shown that chaotic states coexist with regular ones, such as those that describe excitations of the CH bonds. Classical mechanics predict that this is the generic picture for molecules, and this and previous work demonstrate that periodic orbits is a tool to reveal which regions of phase space are regular and which chaotic in connection with the intramolecular motions.

One can move a step further from a qualitative prediction of possible localized states by estimating their energies using a semiclassical trace formula. Although questions about the convergence of this equation always remain, since it is difficult to isolate individual levels, we have argued that Gutzwiller's formula or other versions of it are able to predict low resolution feature states.

Another important outcome of the periodic orbit method is the discovery of those states that are associated with rotating periodic orbits. We have confirmed that saddle-node bifurcations exist above the saddle of the potential function of acetylene as was found for triatomic molecules.[35] The importance of these periodic orbits is that they connect remote regions of phase space and bring stability in an otherwise highly chaotic area.

To recapitulate, the detailed periodic orbit analysis of the C_2H_2 molecular system has shown that for acetylene stable regions in phase space associated with all normal modes remain for high energies. Particularly, the family of periodic orbits that describe CH symmetric stretch motion is stable for more than 30000 cm^{-1}. Considering wave packets trapped in these regular regions, something which is supported from the results of classical survival probability functions, we can understand the regularity of low resolution spectra.

The region of the transition state that separates acetylene and vinylidene is unstable. However, we have located periodic orbits that describe the full rotation of the hydrogen atoms around the CC molecule, and connected them with saddle-node bifurcations. Finally, an investigation for the validity of Gutzwiller's equation in producing feature states was also undertaken for acetylene.

In the light of the above results we may conclude that the extension of the periodic orbit analysis to larger polyatomic molecules and the search for localized high vibrational levels is feasible, and we shall pursue it in the future.

Acknowledgment

We would like to thank Dr. M. Founargiotakis for many fruitful discussions during the course of this project.

Appendix

For completeness of this article we tabulate the commonly used coordinate systems and hamiltonians of tetratomic molecules. J stands for the total angular momentum.

1. **In plane coordinate system**[16] ($J = 0$).

   In this system the hamiltonian has the form:

$$
\begin{aligned}
H \;=\; & \frac{P_R^2}{2M} + \frac{P_{r_1}^2}{2m} + \frac{P_{r_2}^2}{2m} \\
& + \frac{P_{\theta_1}^2}{2}\left(\frac{1}{mr_1^2} + \frac{1}{MR^2}\right) \\
& + \frac{P_{\theta_2}^2}{2}\left(\frac{1}{mr_2^2} + \frac{1}{MR^2}\right) \\
& + \frac{P_{\theta_1} P_{\theta_2}}{MR^2} + V\left(r_1, r_2, R, \theta_1, \theta_2\right), \qquad \text{A1}
\end{aligned}
$$

   where the reduced masses are

$$
\begin{aligned}
M &= \mu_{CC} = \frac{m_C}{2} \\
m &= \mu_{H,HCC} = \frac{m_H\left(m_H + 2m_C\right)}{M_T} \\
M_T &= 2\left(m_H + m_C\right).
\end{aligned}
$$

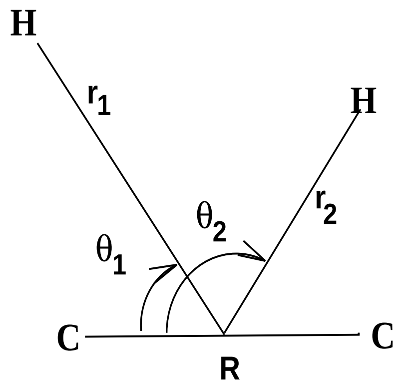

Fig. A1 The coordinate system for the in plane motions (5D).

2. **Jacobi cartesian coordinate system (J may be $\neq 0$).**

$$
\begin{aligned}
H \;=\; & \frac{1}{2\mu_{CC}} \sum_{i=1}^{3} P_i^2 + \frac{1}{2\mu_{H,CC}} \sum_{i=1}^{3} P_{i+3}^2 \\
& + \frac{1}{2\mu_{H,HCC}} \sum_{i=1}^{3} P_{i+6}^2 + V\left(Q_i, Q_{i+3}, Q_{i+6}\right), \qquad \text{A2}
\end{aligned}
$$

where the reduced masses are defined before, and

$$\mu_{H,CC} = \frac{2m_C m_H}{2m_C + m_H}.$$

The generalized coordinates $Q_i (i = 1, \ldots, 12)$ are defined with respect to the space fixed Cartesian coordinate system q_i

$$\begin{aligned}
Q_i &= q_{i+6} - q_{i+3} \\
Q_{i+3} &= q_{i+9} - \frac{m_C q_{i+3} + m_C q_{i+6}}{2m_C} \\
Q_{i+6} &= q_i - \frac{m_C q_{i+3} + m_C q_{i+6} + m_H q_{i+9}}{2m_C + m_H} \\
Q_{i+9} &= \frac{m_H q_i + m_C q_{i+3} + m_C q_{i+6} + m_H q_{i+9}}{M_T}, \quad (i = 1, 2, 3)
\end{aligned}$$

where $Q_{i+9} (i = 1, 2, 3)$ are the Cartesian coordinates of the center of mass of the four atom system. $P_i (i = 1, \ldots, 12)$ are the conjugate momenta of the coordinates $Q_i (i = 1, \ldots, 12)$,

$$\begin{aligned}
p_i &= P_{i+6} + \frac{m_H}{M_T} P_{i+9} \\
p_{i+3} &= -P_i - \frac{m_C}{2m_C} P_{i+3} - \frac{m_C}{2m_C + m_H} P_{i+6} + \frac{m_C}{M_T} P_{i+9} \\
p_{i+6} &= P_i - \frac{m_C}{2m_C} P_{i+3} - \frac{m_C}{2m_C + m_H} P_{i+6} + \frac{m_C}{M_T} P_{i+9} \\
p_{i+9} &= P_{i+3} - \frac{m_H}{2m_C + m_H} P_{i+6} + \frac{m_H}{M_T} P_{i+9}, \quad (i = 1, 2, 3)
\end{aligned}$$

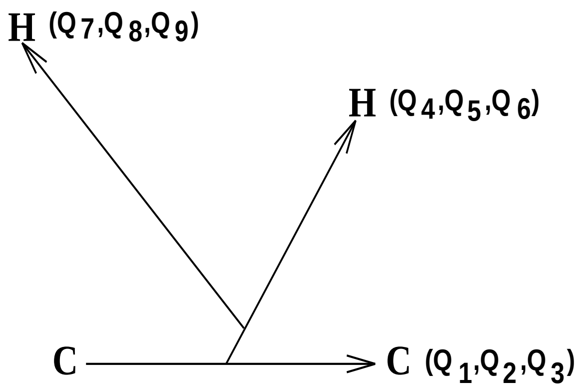

Fig. A2 Jacobi cartesian coordinate system (9D).

3. **Jacobi coordinate system ($J = 0$).**

$$H = \frac{P_{r_1}^2}{2\mu_{H,CC}} + \frac{P_{r_2}^2}{2\mu_{H,HCC}} + \frac{P_R^2}{2\mu_{CC}} + \frac{P_{\theta_1}^2}{2}\left(\frac{1}{I_{r_1}} + \frac{1}{I_R}\right)$$

$$
\begin{aligned}
&+\frac{P_{\theta_2}^2}{2}\left(\frac{1}{I_{r_2}}+\frac{\cos^2\phi}{I_{r_1}\sin^2\theta_1}+\frac{1}{I_R}\left(\cos\phi\cot\theta_1-\sin^2\phi\right)\right)\\
&+\frac{P_\phi^2}{2}\left(\frac{1}{I_{r_2}\sin^2\theta_2}+\frac{1}{I_R}+\frac{\sin\phi\cot\theta_1\cot^2\theta_2}{I_R}\left(2\cos\phi+\sin\phi\cot\theta_1\right)\right)\\
&+\frac{P_\phi^2}{2}\cot^2\theta_2\left(\frac{\sin^2\phi}{I_{r_1}\sin^2\theta_1}+\frac{\cos^2\phi}{I_R}\right)\\
&+P_{\theta_2}P_\phi\left(\frac{\cot\theta_1\cot\theta_2}{I_R}\left(\sin^2\phi-\cos^2\phi-\cos\phi\sin\phi\cot\theta_1\right)\right)\\
&+P_{\theta_2}P_\phi\cot\theta_2\sin\phi\cos\phi\left(\frac{1}{I_R}-\frac{1}{I_{r_1}\sin^2\theta_1}\right)\\
&-\frac{P_{\theta_1}P_\phi}{I_R}+V\left(r_1,r_2,R,\theta_1,\theta_2,\phi\right), \qquad \text{A3}
\end{aligned}
$$

where $\mu_{H,CC}$, $\mu_{H,HCC}$, and μ_{CC} are reduced masses defined before. $I_{r_1} = \mu_{H,CC}r_1^2$, $I_{r_2} = \mu_{H,HCC}r_2^2$, and $I_R = \mu_{CC}R^2$ are the molecular moments of inertia.

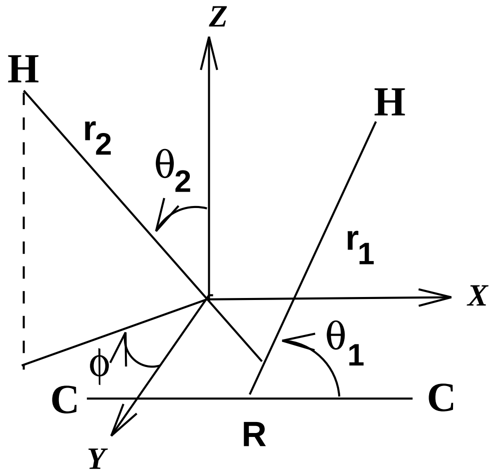

Fig. A3 Jacobi coordinate system (6D).

4. **Diatom-diatom coordinate system ($J = 0$).**[36]

$$
\begin{aligned}
H \;=\;& \frac{P_{r_1}^2}{2\mu_{CH}}+\frac{P_{r_2}^2}{2\mu_{CH}}+\frac{P_R^2}{2\mu_{CH,CH}}\\
&+\frac{P_{\theta_1}^2}{2}\left(\frac{1}{I_1}+\frac{1}{I_{12}}\right)+\frac{P_{\theta_2}^2}{2}\left(\frac{1}{I_2}+\frac{1}{I_{12}}\right)\\
&+\frac{P_\phi^2}{2}\left(\frac{1}{I_2\sin^2\theta_2}+\frac{1}{I_1\sin^2\theta_1}+\frac{2\cos\phi\cot\theta_1\cot\theta_2}{I_{12}}+\frac{(\cot^2\theta_1+\cot^2\theta_2)}{I_{12}}\right)
\end{aligned}
$$

$$-\frac{P_{\theta_1}P_{\theta_2}\cos\phi}{I_{12}}+\frac{P_{\theta_1}P_{\phi}\sin\phi\cot\theta_2}{I_{12}}+\frac{P_{\theta_2}P_{\phi}\sin\phi\cot\theta_1}{I_{12}}$$
$$+V\left(r_1,r_2,R,\theta_1,\theta_2,\phi\right), \qquad \text{A4}$$

where μ_{CH}, and $\mu_{CH,CH}$ are the reduced masses defined by

$$\begin{aligned}\mu_{CH} &= \frac{m_C m_H}{m_C+m_H}\\ \mu_{CH,CH} &= \frac{\left(m_C+m_H\right)^2}{M_T}.\end{aligned}$$

and $I_1=\mu_{CH}r_1^2$, $I_2=\mu_{CH}r_2^2$, and $I_{12}=\mu_{CH,CH}R^2$ are the molecular moments of inertia.

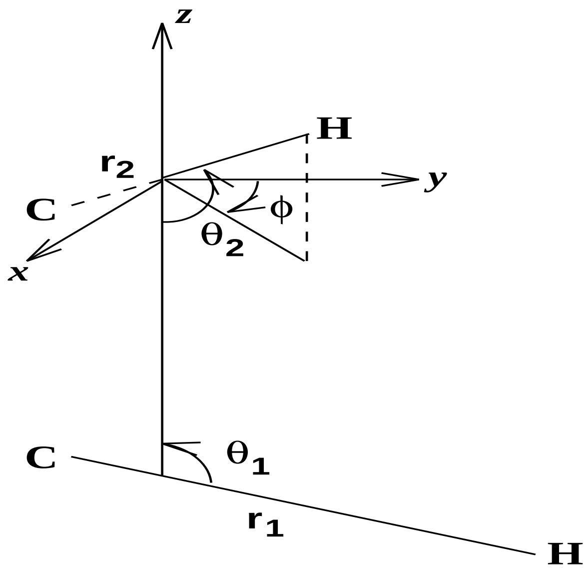

Fig. A4 Diatom-Diatom coordinate system (6D).

References

[1] J. M. G. Llorente and E. Pollak, Ann. Rev. Phys. Chem. **43**, 91 (1992).

[2] J. Tennyson, Rep. Prog. Phys. **58**, 421 (1995).

[3] S. C. Farantos, Int. Rev. Phys. Chem. , in press (1995).

[4] K. Yamanouchi, N. Ikeda, S. Tsuchiya, D. M. Jonas, J. K. Lundberg, G. W. Adamson, and R.W. Field, J. Chem. Phys. **95**, 6330 (1991).

[5] D. M. Jonas, S. A. Solina, B. Rajaram, R. J. Sibey, R.W. Field, K. Yamanouchi, and S. Tsuchiya, J. Chem. Phys. **99**, 7350 (1993).

[6] M. C. Gutzwiller, *Chaos in Classical and Quantum Mechanics*, volume 1, Springer-Verlag, 1990.

[7] O. Bohigas, M.-J. Giannoni, and C. Schmidt, *Quantum Chaos and Statistical Nuclear Physics, Lecture Notes in Physics*, volume 263, Springer - Verlag, 1986.

[8] E. Abramson, R. W. Field, D. Imre, K. K. Innes, and J. L. Kinsey, J. Chem. Phys. **83**, 453 (1985).

[9] L. Leviandier, M. Lombardi, and J. P. Pique, Phys. Rev. Letters **56**, 2449 (1986).

[10] J. P. Pique, J. Opt. Soc. Am. B **7**, 1816 (1990).

[11] E. J. Heller, Acc. Chem. Res. **14**, 368 (1981).

[12] G. J. Scherer, K. K. Lehmann, and W. Klemperer, J. Chem. Phys. **78**, 2817 (1983).

[13] M. Herman, M. A. Temsamani, D. Lemaitre, and J. V. Auwera, Chem. Phys. Letters **185**, 220 (1991).

[14] B. C. Smith and J. S. Winn, J. Chem. Phys. **94**, 4120 (1991).

[15] L. Halonen, M. S. Child, and S. Carter, Mol. Phys. **47**, 1097 (1982).

[16] J. Bentley, R. E. Wyatt, M.Menou, and C. Leforestier, J. Chem. Phys. **97**, 4255 (1992).

[17] E. L. Sibert and R. C. Mayrhofer, J. Chem. Phys. **99**, 937 (1993).

[18] M. J. Bramley and N. C. Handy, J. Chem. Phys. **98**, 1378 (1993).

[19] R. Kosloff, Annu. Rev. Phys. Chem. **45**, 145 (1994).

[20] R. Prosmiti, S. C. Farantos, and H. S. Taylor, Mol. Phys. **82**, 1213 (1994).

[21] E. J. Heller and M. J. Davis, J. Phys. Chem. **84**, 1999 (1980).

[22] E. J. Heller, Phys. Rev. Letters **53**, 1515 (1984).

[23] T. A. Holme and R. D. Levine, J. Chem. Phys. **89**, 3379 (1988).

[24] T. A. Holme and R. D. Levine, Chem. Phys. **131**, 169 (1989).

[25] S. C. Farantos, J. Chem. Phys. **85**, 641 (1986).

[26] R. Seydel, *From Equilibrium to Chaos: Practical bifurcation and stability analysis*, Elsevier, 1988.

[27] S. C. Farantos, in *Time Dependent Quantum Mechanics: Experiments and Theory*, edited by J. Broeckhove, Plenum Co. Ltd, 1992.

[28] M. Founargiotakis, S. C. Farantos, G. Contopoulos, and C. Polymilis, J. Chem. Phys. **91**, 1389 (1989).

[29] S. C. Farantos, M. Founargiotakis, and C. Polymilis, Chem. Phys. **135**, 347 (1989).

[30] S. C. Farantos and H. S. Taylor, J. Chem. Phys. **94**, 4887 (1991).

[31] L. Zachilas and S. C. Farantos, Chem. Phys. **154**, 55 (1991).

[32] S. C. Farantos, and L. Zachilas, Mol. Phys. **80**, 1499 (1993).

[33] W. H. Press, B. P. Flannery, S. A. Teukolsky, and W. T. Vetterling, *Numerical Recipes*, Cambridge Univ. Press, 1986.

[34] E. Reithmeier, *Periodic Solutions of Nonlinear Dynamical Systems*, Lecture Notes in Mathematics, Springer-Verlag, 1991.

[35] S. C. Farantos, THEOCHEM J. Mol. Struct. , in press (1995).

[36] X. Chapuisat, A. Nauts, and G. Durand, Chem. Phys. **56**, 91 (1981).

[37] J. N. Murrell, S. Carter, S. C. Farantos, P. Huxley, and A. J. C. Varandas, *Molecular Potential Energy Functions*, Wiley and Sons, 1984.

[38] A. Weinstein, Inv. Math. **20**, 47 (1973).

[39] J. Moser, Commun. Pure Appl. Math. **29**, 727 (1976).

[40] G. Contopoulos, S. C. Farantos, H. Papadaki, and C. Polymilis, Phys. Rev. E **50**, 4399 (1994).

[41] S. C. Farantos, Chem. Phys. **159**, 329 (1992).

[42] J. M. Gomez Llorente and H. S. Taylor, J. Chem. Phys. **91**, 953 (1989).

[43] J. M. Gomez Llorente, H. S. Taylor, and E. Pollak, Phys. Rev. Letters **62**, 2096 (1989).

[44] S. C. Farantos, J. M. Gomez Llorente, O. Hahn, and H. S. Taylor, J. Chem. Phys. **93**, 76 (1990).

[45] J. F. Stanton, C. Huang, and P. G. Szalay, J. Chem. Phys. **101**, 356 (1994).

[46] M. V. Berry, and M. Tabor, Proc. Royal Soc. London A **349**, 101 (1976).

[47] R. Balian and C. Bloch, Ann. Phys. **85**, 514 (1974).

[48] W. H. Miller, J. Chem. Phys. **63**, 996 (1975).

[49] H. Friedrich and D. Wintgen, Phys. Reports **183**, 37 (1989).

[50] E. Bogomolny and C. Schmit, Nonlinearity **6**, 523 (1993).

[51] M. J. Davis, J. Chem. Phys. **98**, 2614 (1993).

Figure Legends

1. Projection of the bifurcation diagram in (E, p_{r_1}) plane showing the principal families of periodic orbits and bifurcations of them associated with the planar vibrational modes. The symbols denote the symmetric stretch (SS), the anti-symmetric stretch (AS), the carbon carbon stretch (CC), the *trans* bend (TR), and the *cis* bend (CIS) families. Continuous lines mark stable periodic orbits, dotted lines correspond to single unstable periodic orbits, open circles to double unstable orbits, and crosses to complex unstable orbits. Energies are counted from the minimum of acetylene.

2. Plots of representative periodic orbits of acetylene projected in the (r_1, θ_1) plane.

3. Projection of the bifurcation diagram of the principal families of periodic orbits of vinylidene. Diamond symbols represent triple unstable periodic orbits. Energies are counted from the minimum of acetylene.

4. Plots of representative periodic orbits of vinylidene projected in the (r_1, θ_1) plane.

5. Bifurcation diagram of the principal families emanated from the transition state.

6. Plots of representative periodic orbits of the transition state projected in the (r_1, θ_1) plane.

7. Bifurcations diagram showing the saddle-node bifurcations found above the transition state of the isomerization acetylene-vinylidene.

8. Plots of representative saddle-node periodic orbits projected in the (r_1, θ_1) plane.

9. The evolution of the eigenvalues of the monodromy matrix for the periodic orbits R3B2A in the energy range of 28555 - 33288 cm^{-1}. The arrows denote the genesis of complex instability. Figure 9b magnifies the center of Fig. 9a.

10. The classical time autocorrelation functions with initial Gaussian distributions centered on periodic orbits of acetylene and with peak energy 20543 cm^{-1}.

11. As Fig. 10 but for the energy of 28689 cm^{-1}.

12. As Fig. 10 but for vinylidene at energy of 20543 cm^{-1}.

13. As Fig. 10 but for rotating type periodic orbits. The peak energies are in (R1A) 20543 cm^{-1}, and (R3A) 28689 cm^{-1}.

14. The fluctuating part of the density of states of C_2H_2 calculated with Gutzwiller's semiclassical formula. $N(E)$ is produced by using all the in plane principal families of periodic orbits. The vertical lines denote the experimentally assigned feature states with mainly CC stretch $m, (m = 0 - 8)$, and *trans* bend $n, (n = 0 - 18)$, vibrational quantum numbers.

15. The fluctuating part of the density of states constructed by using only the CC and TR families of periodic orbits. The vertical lines denote the experimentally assigned feature states by Yamanouchi et al.,[4] $(m, n), m = 0-8$ and $n = 8-18$. The star signs mark the peaks produced by the CC family only. The broad peaks below the stick spectrum was produced by using Gaussian smoothing functions (see text).